8th U. S. National Combustion Meeting
Organized by the Western States Section of the Combustion Institute
and hosted by the University of Utah
May 19-22, 2013

Reducing minimum flash ignition energy of Al microparticles by addition of WO_3 nanoparticles

Yuma Ohkura[1], *Pratap M. Rao*[1], *In Sun Cho*[1], *and Xiaolin Zheng*[1]

[1]*Department of Mechanical Engineering, Stanford University, Stanford, CA 94305*

Aluminum (Al) due to the large volumetric densities, earth abundance, and low cost, has broad applications in propulsion, thermal batteries, waste disposal and power generation for micro systems. Reducing the sizes of reactive materials down to the nanoscale have been shown to be effective in increasing their reaction rates and reducing their ignition delays. In this study, we demonstrate and understand the flash ignition of Al nanoparticles (NPs), and extending the flash ignition to Al microparticles (MPs) by addition of WO_3 NPs. Nonintrusive optical flash ignition is attractive for many applications due to its simplicity, and flexibility in controlling the area exposed to the flash. However, the oxidation mechanism of Al NPs at large heating rate remains inconclusive due to the lack of direct experimental evidence. We studied the oxidation mechanism of Al NPs under large heating rate (on the order of 10^6 K/s or higher) by a simple flash ignition method, which uses a xenon flash to ignite Al NPs. The flash ignition occurs when the Al NPs have suitable diameters and sufficient packing density to cause a temperature rise above their ignition temperatures. We then extended the flash ignition to Al MPs, which is challenging due to their higher minimum flash ignition energy originating from weaker light absorption and higher ignition temperature compared to Al NPs. By the addition of WO_3 NPs to Al MPs, the minimum flash ignition energy of Al MPs was reduced and we studied the roles of WO_3 NPs upon flash ignition.

1. Introduction

Aluminum is an important fuel for various propulsion systems due to its large energy density (83.8 kJ/cm^3) [1], twice as high as that of gasoline (34.2 kJ/cm^3). For micron-sized Al particles, their combustion process is similar to that of liquid droplet combustion (d^2 law) [2] and the oxidation process occurs after the melting of the outer aluminum oxide. On the other hand, Al nanoparticles (NPs), comparing to micron-sized Al particles, have much lower ignition temperature (~900K) [3, 4], faster burning rates (~2400 m/s) [5] and have the potential to improve the performance of various propulsion systems. However, in field of energetic materials, it remains a challenge to develop a reliable ignition method for practical utilization of the fuel and achieving distributed ignition at multiple locations, thereby can increase reliability of ignition. Especially for Microelectromechanical systems (MEMS) applications, the small fuel quantity and feature size impose a challenge for reliable ignition with common ignition methods requiring physical contact, such as hotwires, heaters and piezoelectronic igniters [6]. Optical ignition by flash, instead, is very attractive because it works without physical contact and can easily achieve distributed ignition at multiple locations, thereby increasing reliability of ignition and flexibility of design. Herein, we applied a flash ignition method [7-11] to Al NPs to study their oxidization behavior at high heating rates. We have also extended the flash ignition to Al MPs. Compared to Al NPs, it is difficult to ignite Al MPs by flash due to their low light absorption and high ignition temperature, and ignition is only possible with a large flash energy (> 1 J/cm^2 from a xenon flash lamp). From a practical point of view, Al MPs are more suitable for engineering systems since they are 30 – 50 times cheaper, safer to handle, and contain much higher Al content due to the much smaller fraction of dead volume and weight of the inert Al_2O_3 shell [12]. Previous work on the combustion of Al MPs has shown that Al MPs burn much faster with the addition of nanoscale metal oxides [13]. Therefore, we extended the flash ignition to Al MPs by adding WO_3 NPs. We observe that the minimum flash ignition energy (E_{min}) of Al MPs is greatly reduced by adding WO_3 NPs, and investigate the effect of WO_3 NPs addition.

2. Methods

Flash ignition of Al NPs and Al MPs are achieved by using a commercial camera flash (Vivitar 285HV and AlienBees™ B1600 Flash Unit), which is equipped with a xenon lamp. A schematic of the flash ignition experimental setup is shown in Figure 1a. Specifically, tens of milligrams of Al powder was placed on top of a 1 mm thick glass slide that was placed directly above the xenon lamp in air. For each flash ignition experiment, the powders are gently packed into a cylindrical shape (diameter: 6.8 mm, height: 2.6 mm) to maintain the same volume and cross-section area exposed to the flash (Figure 1b). We prepared 80 nm Al NPs (SkySpring International Inc.) and two different sizes of Al MPs, *i.e.*, 2.3 μm (Atlantic Equipment Engineers) and 0.9 μm (Sigma-Aldrich). Although the Al NPs are ignited by a single exposure of a xenon flash, flash ignition of Al MPs was not observed under the maximum flash energy of under 0.84 J/cm^2 per flash. To extend the flash ignition from nano to micron scale particles, WO_3 NPs were added to Al MPs. Mixtures of Al MPs and WO_3 NPs are prepared by ultra-sonication using dimethylformamide (DMF) as a solvent. To study the efficacy of WO_3 NP-assisted flash ignition on Al MPs of different sizes, are separately mixed with WO_3 NPs. Al MPs and WO_3 NPs (80 nm, SkySpring Nanomaterials, Inc) are each weighed to satisfy the targeted fuel/oxidizer equivalence ratio while keeping a total mass of 0.530 g. The Al MP and WO_3 NP mixture is added to 10 ml of DMF and sonicated for 15 mins to ensure uniform mixing. After sonication, the mixture is gently dried on a hotplate at 100 ^oC for 6 hours to remove the DMF. Finally, the dried mixture powder is passed through a 140 mesh (105 μm) sieve to break up large agglomerates. The Al-to-WO_3 equivalence ratio (ϕ) and normalized equivalence ratio (ϕ_n) of the mixture are defined in Equation (1),

$$\phi = \frac{\left(\frac{m_{Al}}{m_{WO3}}\right)}{\left(\frac{m_{Al}}{m_{WO3}}\right)_{st}}, \quad \phi_n = \frac{\phi}{1+\phi} \tag{1}$$

, where m_{Al} and m_{WO3} refer to the mass of Al and WO_3, and the subscript *st* refers to the stoichiometric condition for the reaction $2Al + WO_3 \rightarrow Al_2O_3 + W$. Although the Al MPs are encapsulated by a native inert Al_2O_3 shell (2 - 5nm), the active Al content is 97.5 % for the small (0.9 μm) and 99.0 % for large (2.3 μm) Al MPs with a 5 nm shell. Hence, we assume that the entire mass of the Al MPs is Al when calculating the equivalence ratios. To measure the E_{min}, the power of the flash is increased gradually until flash ignition occurs. Flash ignition experiments are carried out both in air and in N_2 atmospheres. For the flash ignition experiments in N_2, the entire flash unit and samples are placed inside an inflatable polyethylene glove box (Atmosbag glove bag, Sigma-Aldrich) that is purged constantly with 99.95 % pure N_2.

The wavelength-dependent light absorption properties of various mixture samples are obtained with an integrating sphere using a xenon lamp coupled to a monochromator (Model QEX7, PV Measurements, Inc.). For the reflectance (R %) measurement, the samples are mounted at the backside of the integrating sphere and the reflectance spectra are normalized to the reflection of a white-standard. The transmittance spectra (T %) are obtained by comparing the transmittance of test samples with a calibrated Si reference photodiode. The absorption (A %) is calculated with the formula, A % = 100 % - T % - R %.

3. Results and Discussion

3.1 Flash ignition of Al particles

The Al NPs ignited by a single exposure of a xenon flash (Figure 1b) burn in air for about 10 seconds with a yellow glow (Figure 1b, inset). The Al NPs change from dark gray, loose powders to light gray aggregated particles after combustion (Figure 2a). The original Al NPs, viewed under the scanning electron microscope (SEM, FEI XL30 Sirion, 5 kV), are spherical and highly agglomerated with an average diameter in the range of 60 to 96 nm (Figure 2b) with a 2 nm thick native aluminum oxide layer and, after flash ignition, they are oxidized into much smaller NPs (3 - 20 nm, Figure 4i), which are agglomerated (Figure 2c). It should be noted that flash ignition of Al NPs was not observed when NPs were placed sparsely over the glass slide by drop casting Al NPs diluted with hexane onto the slide and then allowing the hexane to evaporate. The results of the above experiments suggest that the packing density and the diameter of Al particles are important factors for successful flash ignition.

In the case of Al MPs, optical images in Figure 2d show the sample appearance before and after the flash ignition in air, where the sample is a stoichiometric mixture of Al MPs (2.3 μm) and WO_3 NPs (80 nm) with $\phi = 1$. After ignition, the mixture color changes from gray to dark blue. The dark blue color indicates that some WO_3 (yellow) is reduced to WO_{3-x} (blue), and not completely to W (silver or gray color). The sample is spread out over a larger area after ignition, suggesting a violent reaction that is accompanied with gas expansion. Before flash ignition, Figure 2e shows that the spherical Al MPs (2.3 μm) and the WO_3 NPs are mixed, forming a densely packed powder. After the flash ignition, the products form much larger particles that are tens of microns in size (Figure 2f), suggesting that melting and fusion occur

together with reaction. The characterizations confirm that reaction has occurred between Al MPs and WO_3 NPs upon exposure to a single optical flash. Flash ignition occurs when the energy of the incident light absorbed by the mixture of Al MPs/WO_3 NPs is sufficient to raise the mixture temperature beyond its ignition temperature.

3.2 Estimation of the temperature increase of Al particles

To further investigate Al particle flash ignition, we estimated the temperature increase of Al particles by a single flash exposure. The flash ignition of Al particles is achieved by the photo-thermal effect, when the energy of the incident light absorbed by Al particles is sufficient to raise their temperatures beyond their ignition temperatures. The purpose of the calculation is to simulate the initial stage of flash ignition and to understand the qualitative dependence of temperature rise on the size and packing density of Al particles. We estimated the temperature rise from room temperature (300 K) of Al particles when exposed to a flash. The spectrum of the camera flash is assumed to be a blackbody radiation at a temperature of 6500 K [14] and the incident light intensity, I_{inc}, is approximately 1000 W/cm^2 on the basis of energy density of 1 J/cm^2 and the flash duration of 1 ms [9, 15]. The light absorption by the Al_2O_3 shell is neglected, since Al_2O_3 is almost optically transparent [16]. Since Al has high thermal conductivity, the temperature distribution inside the Al particle is assumed to be constant. The heat source is the total energy absorption rate P (W) of Al particles by the incident flash light, which is calculated by integrating over the specific energy absorption rate over all the wavelengths λ, ranging from 185 to 2000 nm and corrected with the emissivity factor ($e = I_{inc}/ sT^4$), as shown in Eq. (2)

$$P = \frac{I_{inc}}{\sigma T^4}\int \frac{1}{\lambda^5}\frac{4\pi^2 c^2 \hbar}{\exp[2\pi c\hbar/(\lambda k_B T)]-1} C_{abs}(\lambda) d\lambda \quad , \qquad (2)$$

where σ is the Stefan–Boltzmann constant; c is the speed of light; $\hbar$ is the reduced Planck constant, and k_B is the Boltzman constant. The specific energy absorption rate at a specific wavelength is the product of the absorption cross-section, $C_{abs}(\lambda)$, and the intensity of the incident light at the wavelength. The absorption cross-section $C_{abs}(\lambda)$ was calculated by using a Mie theory calculator "Mieplot" [17].

The temperature rise of Al particles was estimated by assuming that the energy absorbed by the Al particles is used to heat up the particles and the confined air.

$$(\rho_{air} V_{air} c_{p,air} + \rho_{Al} V_{Al} c_{p,Al})\Delta T = p V_{Al} \Delta t \quad , \qquad (3)$$

$$\Delta T = \frac{p\Delta t}{\frac{\rho_{air} c_{p,air}}{\phi} + \rho_{Al} c_{p,Al}} \quad , \qquad (4)$$

where p is the energy absorption rate per unit volume (W/m^3) by Al particles, and Δt is the flash duration (sec). ϕ is the packing density defined as $\phi = V_{Al}/V_{air}$, i.e., the volume ratio of Al particles to the confined air among the particles. Here for estimation purpose, we assumed that the Al and air have the same temperature rise, although the actual temperature of Al will be higher than that of air [18]. We also neglected the optical interactions among Al particles and the possible air expansion between Al particles due to the heating. It should be noted that the estimation presented here is not a rigorous flash heating model, which is far from trivial due to the complexity in describing the Al NP distribution and interfacial heat conductivity, but rather its purpose is to provide qualitative information on the dependence of temperature rise on the size and packing density of Al particles [15].

Figure 3 shows the dependence of the temperature rise of the Al particles on their sizes and packing densities. First, the largest temperature rise is expected for Al particles with approximately 75 nm diameter, regardless of the packing density. As the size of the Al particles increases beyond 75 nm, the temperature rise decreases because the particles absorb less energy. In addition, larger micron Al particles require much higher ignition temperature of above 1200 K [19]. Hence, Al MPs cannot be ignited by a flash. Second, there is a critical Al packing density to achieve flash ignition because, for Al particles of the same diameter, their temperature rise increases sharply with the Al packing density and eventually saturates when the packing density is roughly above 1% (Figure 3, inset). The reason that higher temperature rise is expected for larger packing densities of Al particles is that more heat per unit volume is absorbed. In summary, successful flash ignition of Al particles relies on two important parameters: their diameters and their packing densities.

3.3 Al NP oxidation mechanism

Next, we investigated the oxidation mechanism of Al NPs ignited by a camera flash. Al NPs ignited by the flash are likely to be oxidized by the MDM due to the large heating rate, on the order of 10^6 K/s or higher. To verify the MDM oxidation, we studied the oxidation process of Al NPs in air by examining multiple NPs after the flash exposure using TEM. Due to the intrinsic spatial non-uniformity of the flash light intensity and the packing density of Al NPs, Al NPs will have different temperature rise and exposure to oxygen, so their oxidation process will quench at different stages after the flash exposure. Therefore, by examining many Al NPs, we can re-construct the oxidation process of Al NPs as illustrated in Figure 4. Initially, Al melts upon exposure to the flash, which pushes the oxide shell outwards (Figure 4b, 4f). When the pressure rise associated with the melting of Al is large enough, it ruptures certain regions of the oxide shell and the molten Al flows out (Figure 4c, 4g). Subsequently, Al and oxygen contact with each other and react exothermically. The heat generated further causes more Al to melt or even evaporate, which pushes the oxide shell further out, and the original Al NP has grown from less than 100 nm to over 300 nm in diameter (Figure 4d, 4h). As shown in Figure 4h, the big hollow sphere corresponds to the expanded Al particle and the much smaller solid spheres formed from the core Al remains inside the hollow sphere. Eventually, the entire particle fractures and breaks into clusters of 3 - 20 nm, much smaller than the original Al NPs (Figure 4e, 4i). The clusters consist of both Al_2O_3 particles and partially oxidized Al particles. These observations strongly suggest that the Al NPs ignited by the flash are oxidized by the MDM.

3.4 Reduction of E_{min} of Al MPs by addition of WO_3 NPs

We further extended the flash ignition to Al MPs by addition of WO_3 NPs. WO_3 NPs influence the flash ignition of Al MPs in two ways: i) increasing light absorption and ii) decreasing ignition temperature by supplying oxygen to Al. To quantify the effect of WO_3 NPs, the E_{min} for the mixture of Al MPs and WO_3 NPs is plotted as a function of normalized Al/WO_3 equivalence ratio in both air (black squares) and inert N_2 (red circles) in Figure 5. Figures 5a and 5b correspond to larger Al MPs (2.3 μm) and smaller Al MPs (0.9 μm), respectively. The error bars are established by performing three experiments with identical conditions, and represent the range of measured E_{min} within the three measurements. First, both E_{min} curves (Figure 5a and 5b) show a concave shape, with higher E_{min} values in both the Al lean and rich regions, a trend that is very similar to that of E_{min} for ignition of various gaseous fuel/air mixtures [20]. The lowest point of the E_{min} curve does not correspond to the stoichiometric condition of reaction $2Al + WO_3 \rightarrow Al_2O_3 + W$ ($\phi = 1$, $\phi_n = 0.5$), since WO_3 is not completely reduced to tungsten in the flash experiment. Second, when Al is the deficient species with respect to WO_3 ($\phi_n < 0.5$), E_{min} in air is comparable to that in N_2. The fact that E_{min} does not increase when gaseous O_2 is removed suggests that Al MPs are preferentially oxidized by the WO_3 NPs. WO_3 NPs are more effective oxidizers than air because of their large contact area with the Al MPs, which facilitates ignition through the diffusion-based reactive sintering mechanism [21, 22]. Third, adding WO_3 NPs to pure Al MPs (ϕ_n =1) or to Al MPs in excess supply with respect to WO_3 ($\phi_n > 0.5$), *i.e.*, changing ϕ_n from 1 to 0.5, significantly lowers E_{min} because WO_3 oxidizes Al more effectively than air. Finally, when comparing Al MPs of two different sizes, E_{min} for the 2.3 μm Al MPs is on average 0.4 J/cm^2 higher than that for the 0.9 μm Al MPs, which is consistent with the reported observation of higher ignition temperature of 1600 K for larger (2.3 μm) particles compared to 1400 K for smaller (0.9 um) particles [23, 24]. Nevertheless, addition of WO_3 NPs reduces E_{min} for Al MPs of both sizes.

The above E_{min} measurements show that WO_3 NPs are more effective oxidizers than air for Al MPs. In addition, WO_3 NPs can also enhance the light absorption of the mixture of Al MPs/WO_3 NPs upon flash exposure, which can increase the temperature rise due to the photothermal effect. Figure 6 shows the light absorption spectra of several mixtures of Al MPs and WO_3 NPs over wavelengths of 300 - 1100 nm. Figures 6a and 6b correspond to larger (2.3 μm) and smaller (0.9 μm) Al MPs, respectively. First, for pure Al MPs ($\phi_n = 1.0$), the slight absorption increase around 830 nm corresponds to the inter-band transition frequency of 1.5 eV for aluminum [25]. For all the other samples containing WO_3 NPs, light absorption is clearly increased for wavelengths below 460 nm, consistent with the WO_3 bandgap of 2.7 eV ($\lambda = 460$ nm). Second, the smaller Al MPs absorb about 15 % more light than the larger Al MPs, facilitating the flash ignition process. Third, the total light absorption is calculated by integrating the product of the xenon flash spectrum and the absorption plus scattering spectrum over 300 - 1100 nm wavelengths. The total light absorption is increased by 12.2 % and 1.4 % for the larger (2.3 μm) and smaller (0.9 μm) Al MPs, respectively, when a stoichiometric quantity of WO_3 NPs ($\phi_n = 0.5$) is added to the pure Al MPs. Since the light absorption enhancement due to the addition of WO_3 NPs is negligible for the smaller Al MPs, the reduction in E_{min} is mainly attributed to effective oxygen supply by WO_3 NPs due to their intimate and large contact area with Al MPs. On the other hand, for larger Al MPs, the reduction of E_{min} by WO_3 addition results from both effective oxygen supply and enhanced light absorption.

4. Conclusions

We have demonstrated that Al NPs and MPs can be ignited by a camera flash through the photo-thermal effect. Flash ignition has the advantages of low power input, multi-point initiation and broad spectrum emission. Our analysis reveals that successful flash ignition requires Al particles to have a suitable submicron diameter range and a large packing density, in order to achieve sufficient temperature rise. Furthermore, TEM analysis of Al NPs after the flash exposure air suggests that Al NPs are oxidized through the Melt-Dispersion Mechanism, which is the first direct experimental observation thereof. We also have extended the flash ignition to Al MPs and studied the effect of WO_3 NP addition on the flash ignition of Al MPs of two different sizes by measurement of the E_{min}. The E_{min} is greatly reduced by the addition of WO_3 NPs for Al MPs of both sizes. For the smaller Al MPs, the reduction mainly comes from the more effective oxygen supply by WO_3 NPs than by air. For the larger Al MPs, the reduction is due to the combined effects of effective oxygen supply and light absorption enhancement by WO_3 NPs. These results extend the flash ignition of expensive and lower energy density Al NPs to inexpensive and higher energy density Al MPs. The flash ignition may find uses in many engineering applications requiring distributed, nonintrusive and miniaturizable ignition systems in lieu of sparks and hotwire igniters.

Acknowledgements

This work was supported by the Army Research Office under the grant W911NF-10-1-0106. Y.O. acknowledges support from the Japan Student Services Organization Fellowship. P.M.R. acknowledges support from the Link Foundation Energy Fellowship.

References

1. M. C. G. S. H. Fischer, Proc. 24th Int. Pyrotechnics Seminar, Monterey, CA (1998) 1-6
2. M. W. Beckstead, Internal Aerodynamics in Solid Rocket Propulsion (2004) 1-46
3. C. J. T.P. Parr, D. Hanson-Parr, K. Higa, K. Wilson, 39th JANNAF Combustion Subcommittee Meeting (2003)
4. T. T. K. C.J. Bulian, J.A. Puszynski, 31st International Pyrotechnics Seminar, Fort Collins, CO (2004)
5. R. Shende; S. Subramanian; S. Hasan; S. Apperson; R. Thiruvengadathan; K. Gangopadhyay; S. Gangopadhyay; P. Redner; D. Kapoor; S. Nicolich; W. Balas, Propellants, Explosives, Pyrotechnics 33 (2) (2008) 122-130
6. C. Rossi; D. Estève, Sensors and Actuators A: Physical 120 (2) (2005) 297-310
7. P. M. Ajayan; M. Terrones; A. de la Guardia; V. Huc; N. Grobert; B. Q. Wei; H. Lezec; G. Ramanath; T. W. Ebbesen, Science 296 (5568) (2002) 705
8. N. Wang; B. D. Yao; Y. F. Chan; X. Y. Zhang, Nano Letters 3 (4) (2003) 475-477
9. L. J. Cote; R. Cruz-Silva; J. X. Huang, Journal of the American Chemical Society 131 (31) (2009) 11027-11032
10. M. R. Manaa; A. R. Mitchell; R. G. Garza; P. F. Pagoria; B. E. Watkins, Journal of the American Chemical Society 127 (40) (2005) 13786-13787
11. A. M. Berkowitz; M. A. Oehlschlaeger, Proceedings of the Combustion Institute (In Press, Corrected Proof) (2010)
12. V. I. Levitas; M. L. Pantoya; K. W. Watson, Applied Physics Letters 92 (20) (2008)
13. M. R. Weismiller; J. Y. Malchi; J. G. Lee; R. A. Yetter; T. J. Foley, Proceedings of the Combustion Institute 33 (2) (2011) 1989-1996
14. H. K. Aslin, Review of Scientific Instruments 38 (3) (1967) 377
15. N. Zeng; A. B. Murphy, Nanotechnology 20 (37) (2009) 375702
16. Y. A. Akimov; W. S. Koh, Nanotechnology 21 (23) (2010) 235201
17. P. Laven, MiePlot v4.2 software is available at www.philiplaven.com/MiePlot.htm.
18. A. O. Govorov; H. H. Richardson, Nano Today 2 (1) (2007) 30-38
19. M. A. Trunov; M. Schoenitz; E. L. Dreizin, Propellants Explosives Pyrotechnics 30 (1) (2005) 36-43
20. B. Lewis; G. Von Elbe, in: Combustion, flames and explosions of gases, Academic Press: New York, 1987
21. Y. Yang; Z. Sun; S. Wang; D. D. Dlott, The Journal of Physical Chemistry B 107 (19) (2003) 4485-4493
22. E. V. Chernenko; L. F. Afanaseva; V. A. Lebedeva; V. I. Rozenband, Combust Explo Shock+ 24 (6) (1988) 639-646
23. M. A. Trunov; M. Schoenitz; E. L. Dreizin, Combustion Theory and Modelling 10 (4) (2006) 603-623
24. Y. Huang; G. A. Risha; V. Yang; R. A. Yetter, Combustion and Flame 156 (1) (2009) 5-13
25. C. F. Bohren; D. R. Huffman, in: Absorption and Scattering of Light by Small Particles, Wiley-VCH Verlag GmbH: Weinheim, Germany, 1998

Figures

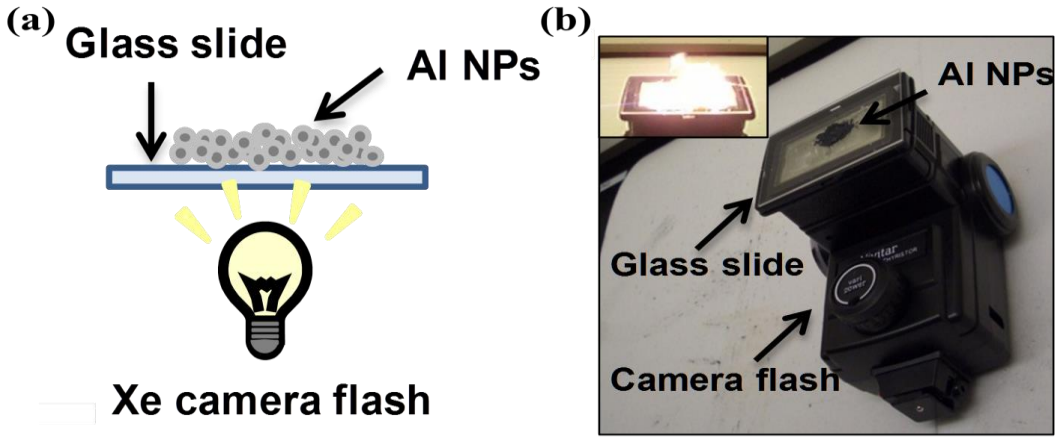

Figure 1: (a) Schematic and (b) optical images of the experimental setup for ignition of Al NPs (80 nm) by a camera flash. Inset: photograph of the burning of flash ignited Al NPs which casts a yellow glow and lasts for about 10 s.

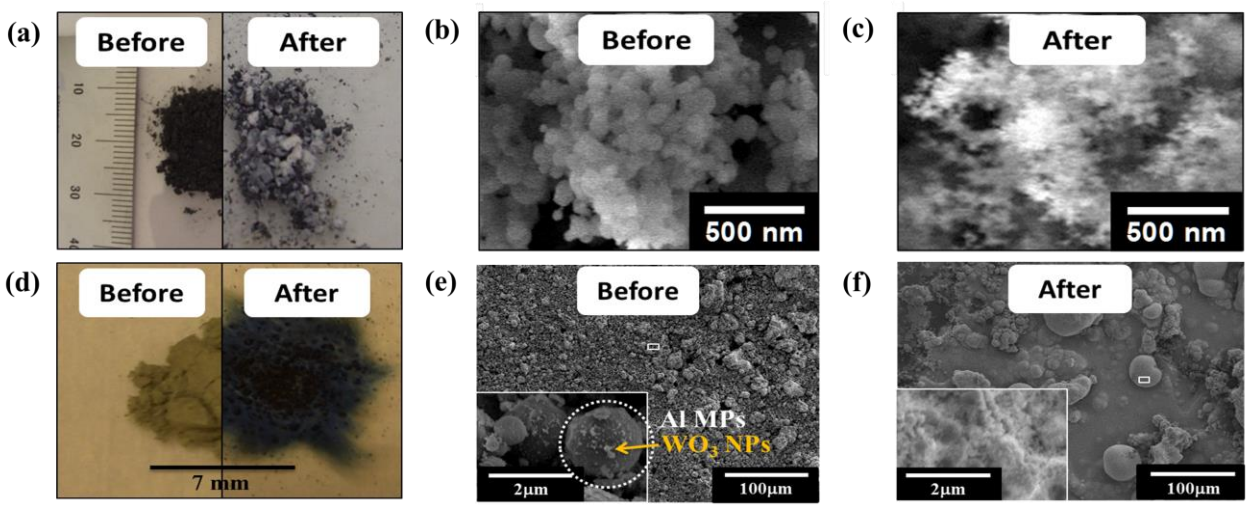

Figure 2: (a–c) Optical and SEM images of Al NPs before and after the exposure. The original spherical Al NPs break up into smaller clusters after burning. (d-f) Optical and SEM images of a mixture Al MPs (2.3 µm) and WO_3 NPs (80 nm). After the flash ignition, the products form much larger particles that are tens of microns in size, suggesting that melting and fusion occur together with reaction.

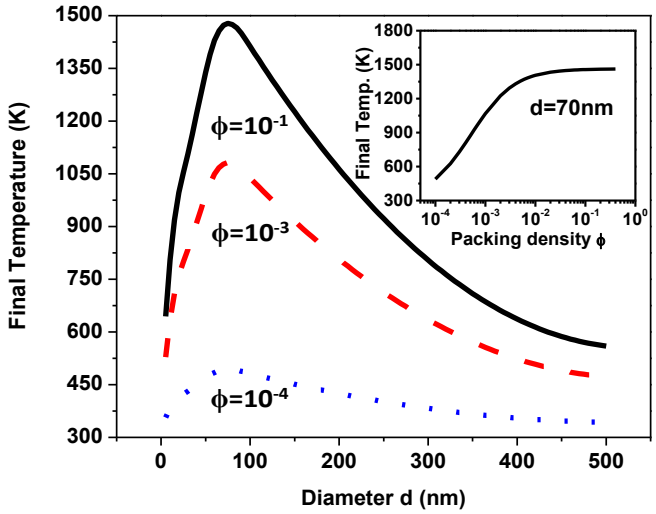

Figure 3: Estimated temperature rise of Al particles by a flash exposure as a function of the Al particle diameter for different packing densities. Inset: The temperature rise of Al NPs with a diameter of 70 nm as a function of the packing density of Al NPs.

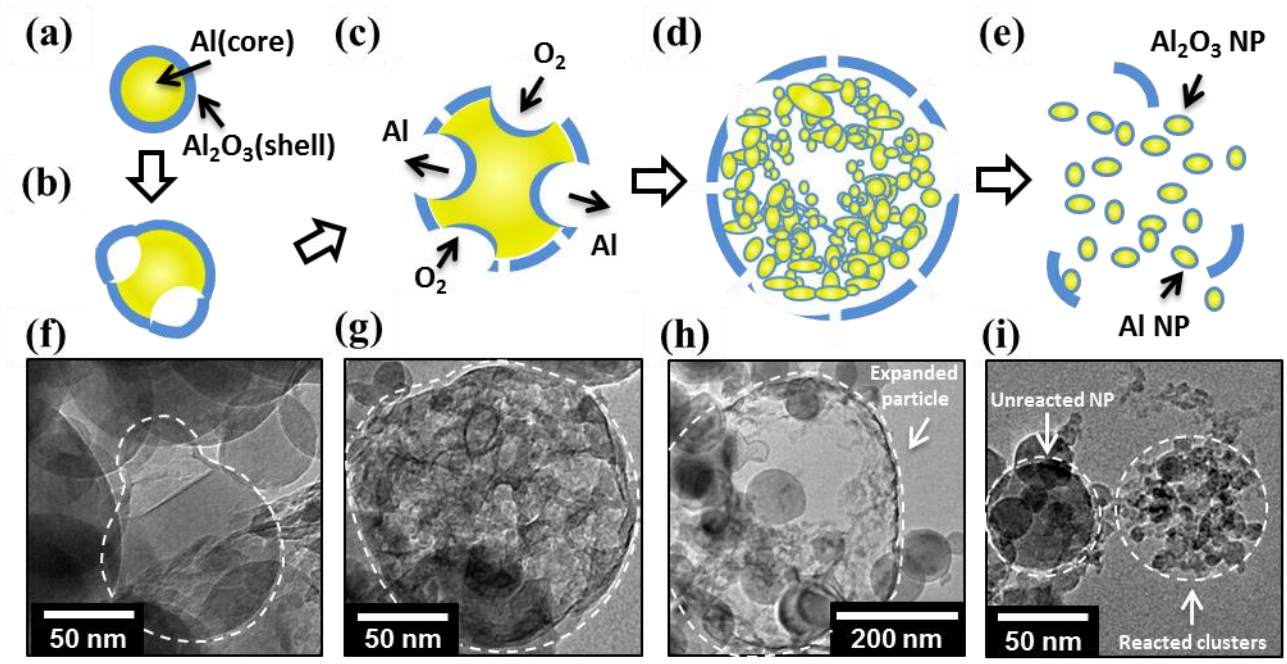

Figure 4: (a - e) Schematics and (f - i**)** TEM images illustrate the oxidation process of the Al NPs when exposed to a flash in air. (a) Initial Al NPs are covered by a Al_2O_3 shell. (b) and (f) Al melts upon rapid heating which pushes the shell outwardly. (c) and (g) the shell ruptures and the melted Al becomes in contact with air. (d) and (i) the large hollow sphere corresponds to the expanded Al NPs, where most Al has flown away from the particle center and been oxidized at the particle surface. (e) and (j), the hollow sphere fractures into small clusters of 3 – 20 nm in sizes. These clusters are consisted of both Al_2O_3 particles and partially oxidized Al particles.

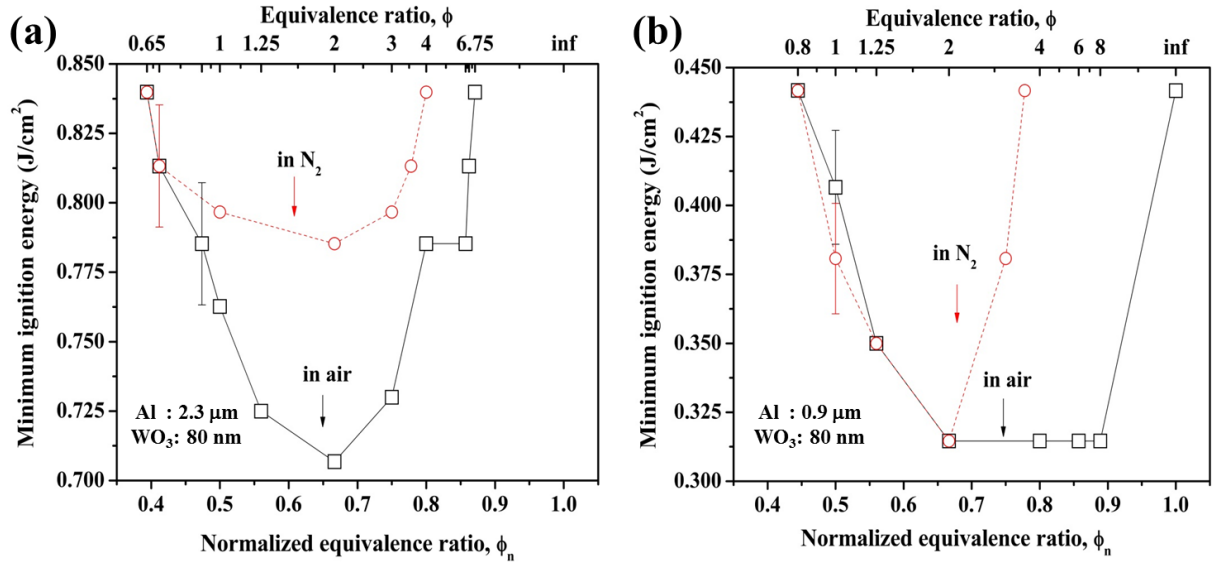

Figure 5: Minimum flash ignition energy of Al MPs with addition of WO_3 NPs. (a) Large Al MPs (2.3 µm) and (b) small Al MPs (0.9 µm) mixed with WO_3 NPs with respect to normalized equivalence ratios in air and nitrogen gas.

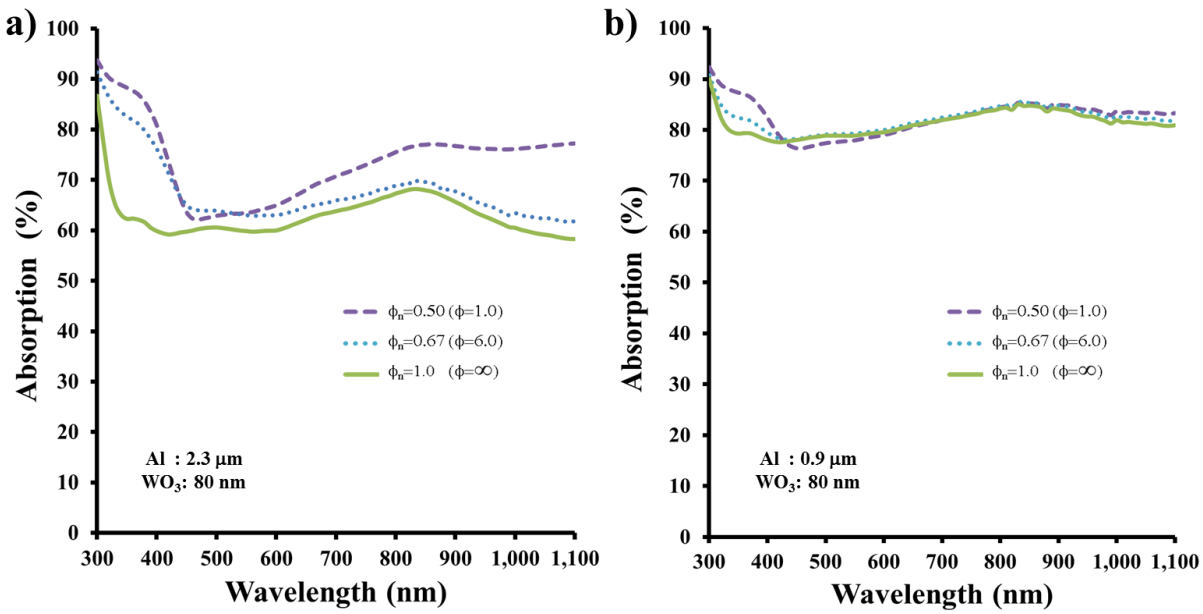

Figure 6: Optical characterizations of Al MPs with addition of WO_3 NPs. Absorption (a) large Al MPs (2.3 μm) and (b) small Al MPs (0.9 μm) mixed with WO_3 NPs with respect to normalized equivalence ratios over a wavelength of 300 - 1100 nm.